Applied Composite Materials (2024) 31:1219–1235
https://doi.org/10.1007/s10443-024-10229-w

RESEARCH

Experimental Method to Determine the Draping Behavior of Auxiliary Materials for the Vacuum Bagging of CFRP Parts on Doubled-Curved Surfaces

Clemens Schmidt-Eisenlohr[1] · Heinz Voggenreiter[1] · Michael Kupke[1]

Received: 8 December 2023 / Accepted: 8 April 2024 / Published online: 3 May 2024

Abstract
The production costs of aircraft primary structures made of carbon fibre reinforced polymer (CFRP) are significantly higher than for comparable metal-based structures. Today substantial effort is made to achieve a sufficient reproducibility and parts' quality in manufacturing processes of CFRP structures. Especially the sub process vacuum bagging for infusion processes is still expensive. One of the reasons is the complex positioning of the flexible auxiliary materials which have to be stacked on the preform. During the positioning on doubled-curved surfaces these materials tend to form wrinkles, which can lead to defects of the composite part. Yet, a defined description of the wrinkling behavior of the auxiliary materials on doubled-curved surfaces does not exist. In this work a characterization of the wrinkling behavior on doubled-curved surfaces is investigated for the auxiliary materials of the Vacuum Assisted infusion Process (VAP®): release film, perforated peel ply, flow media, membrane and vacuum foil. Therefore, an experimental test method is derived similar to established hemisphere deformation test methods. The wrinkling behavior for the specific VAP auxiliary materials is empirically determined on differently curved surface geometries. It is shown that the draping behavior can be characterized by partial wrinkle-free surfaces between the wrinkles. A material specific threshold is derived to determine the appearance of wrinkles. The work shows that a characterization of the draping behavior of auxiliary materials on doubled-curved surfaces is possible. With the gained knowledge the potential for an increase of the vacuum bagging reproducibility is given.

Keywords CFRP · Auxiliary materials · Doubled curvature · Vacuum bagging · Draping behavior · Wrinkle determination

✉ Clemens Schmidt-Eisenlohr
clemens.schmidt-eisenlohr@dlr.de

Heinz Voggenreiter
heinz.voggenreiter@dlr.de

Michael Kupke
michael.kupke@dlr.de

[1] Institute for Structure and Design, German Aerospace Center, Am Technologiezentrum 4, Augsburg 86159, Bavaria, Germany

1 Introduction

Within the last decades the fraction of composite parts within the structure of aircraft increased. Primary structures of the Airbus A350 [1], the Boeing 787 [2] and the Airbus A220 (former Bombardier CSeries) [3] are manufactured using high performance composite parts. One of the established manufacturing processes in industry is a resin infusion process, the Vacuum Assisted Process (VAP®) [4–6]. The VAP® is used in series production of the rear pressure bulkhead of the A350 [7], the wing of the Irkut MS21 [8] and Airbus A220 [9]. A process to produce an infused composite part is subdivided in dry fibre preforming, vacuum bagging, resin infusion and consolidation in a furnace [10]. This article focuses on the vacuum bagging process, in which research work was done to improve, simplify or automate the process. The main function of the vacuum bagging is to encapsulate the preform on the tooling. Vacuum, when applied to the preform enables to infuse the preform with liquid resin. In order to achieve an adequate evacuation of the preform, the vacuum bagging has to provide a sufficient permeability and areal air out-flow. Additionally the vacuum bagging has to ensure a defined surface of the composite part. Wrinkles in the vacuum bagging materials are symptomatic for the vacuum bagging process. The amount of wrinkles increases with the complexity of the parts' shape. In Fig. 1 a typical wrinkle arrangement is shown for the vacuum foil. The arrangement is performed manually and therefore a high amount of effort is needed to arrange and control the wrinkle pattern to achieve a sufficient quality.

The wrinkles can lead to critical defects of the composite part. A reduction of wrinkles would increase the process robustness and therefore reduce production costs, especially for complex shaped composite parts. A prediction method of wrinkles and wrinkle free areas would allow the development of wrinkle reduction strategies and most likely enable automation solutions for vacuum bagging. But a method or simulation to predict the draping and wrinkling behavior of the specific auxiliary materials based on the preform shape does not exist yet.

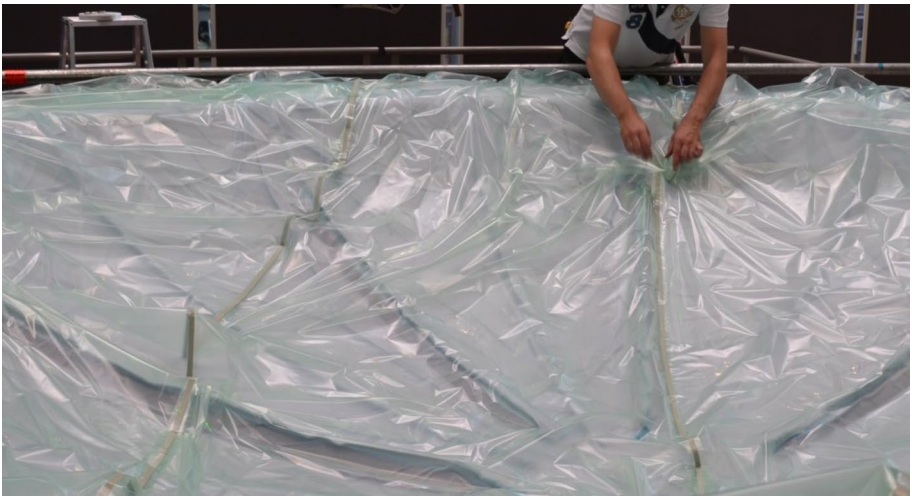

Fig. 1 Wrinkling arrangement during vacuum bagging

2 State of the Art

To perform a vacuum bagging several layers of auxiliary materials need to be stacked on the preform and tooling. After stacking the vacuum bag is sealed and vacuum is applied. Thus the auxiliary materials are compressed and draped to the preforms surface shape. The vacuum bagging for the VAP® can be separated and classified as an inner vacuum bag and an outer vacuum bag (see Fig. 2). The sequence of the auxiliary materials for the inner vacuum bag is peel ply (PP), release film (RF) and flow media (FM). The sequence of the auxiliary materials for the outer vacuum bag is semipermeable membrane (M), distribution media (DM) and vacuum foil (VF) [12].

Auxiliary Materials Each of the auxiliary materials has a specific function in the vacuum bagging process, see following listing:

- Peel ply ensures that the parts surface is properly impregnated with resin and it creates an uniform surface structure for following processing steps, e.g. assembly processes
- Release film enables the demolding of the auxiliary materials after curing without removing the peel ply. The release film is uniformly perforated to allow the resin flow during the infusion process
- Flow media has a high permeability related to the preform even if vacuum is applied. Therefore flow media is used to increase the infusion velocity of the resin which is inevitable to infuse large composite parts
- Semipermeable membrane is permeable for the air flow but blocking for resin. The semipermeable membrane enables the evacuation of the preform over its entire top surface. The application of a semipermeable membrane in the VAP® is the key difference to most of the other infusion processes
- Distribution media has a high permeability related to the preform even if vacuum is applied. Therefore distribution media is used to enable a sufficient areal air-out flow over the entire surface of the semipermeable membrane respectively the preform. In the VAP® process distribution media (DM) is the same material type as flow media (FM). In this article distribution media is subsequently considered by the flow media (FM)

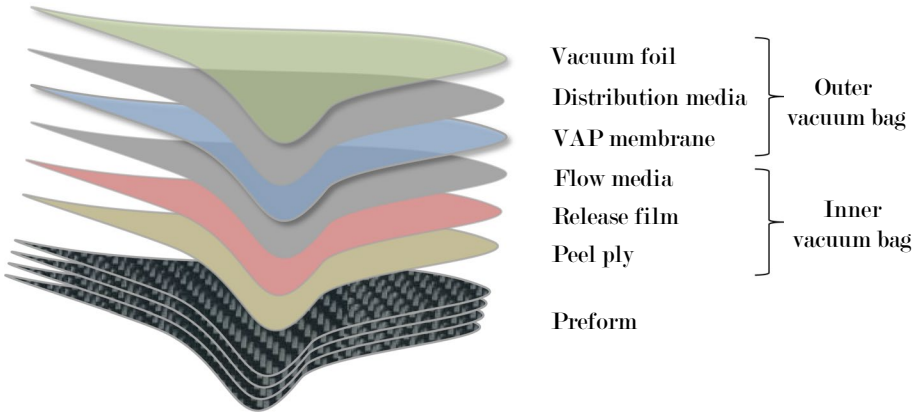

Fig. 2 Stacking sequence of the auxiliary materials with division in an inner and outer vacuum bag [11]

- Vacuum foil completes the vacuum bag on top and is circumferentially sealed to the tooling. Therefore a vacuum can be applied below to evacuate the preform and the other auxiliary materials.

Draping Mechanisms The drapablity of the various auxiliary materials on doubled-curved surfaces differs depending on their dominant draping mechanism. There are two main, material depended draping mechanisms to achieve a wrinkle-free placement of a material on a doubled-curved surface. First, draping by in-plane elongation respectively in-plane compression of the material. Second, draping by in-plane shear of the material. These draping mechanisms can occur in a material during draping at the same time. An additional, application-oriented draping approach is the deformation by partial forming of wrinkles. Wrinkles are necessary if the limits of draping through elongation, compression or shearing are exceeded. The additionally placement of wrinkles is necessary to avoid too high plastic deformations which negatively affect the auxiliary materials function.

The considered auxiliary materials are fabrics or foils [13], thus the draping mechanisms and subsequently the drapability differs from one to the other:

- Peel ply is basically a woven fabric whereat the primarily appearing draping mechanism is shearing which can be used for draping of peel ply.
- Release film is a foil whereat the primarily appearing draping mechanism is elongation. However, release film may be elongated only to a minor degree in order to avoid infusion process critical changes of the hole pattern.
- Flow media and distribution media for complex shaped draping are usually knitted textiles whereat the primarily appearing draping mechanism is shearing, which can be used for draping of the materials.
- For the semipermeable membrane as a combination of a woven fabric coated with a mebrane the draping mechanism is a combination of shearing and elongation. However, the proper functionality of the membrane layer is highly sensitive to elongation and shearing as micro pores are increased and process critical resin passage is enabled.
- Vacuum foil is a foil whereat the primarily appearing draping mechanism is elongation. Vacuum foils have a significantly higher elongation at break which can be used for draping. However, even minor in-plane shearing leads to wrinkling of the foils.

Sancak investigated the shearability of the different auxiliary materials using the picture frame test method [14]. Merely for peel ply the maximum shear angle was determined to $\gamma_{max} = 6°$. For the other auxiliary materials the determination of a maximum shear angle was not feasible due to the sensitivity of the test method. It is not sufficient to detect the low maximum shear angles of these auxiliary materials. Even though Sancak could not determine these maximum shear angles, he estimated that these angles are significantly lower than 6°. In comparison to woven carbon fabrics used for complex preforming the maximum shear angle of the auxiliary materials is significantly lower. The dominant draping mechanism of woven fabrics is in-plane shear [15]. The maximum shear angle depends on the specific web properties and often reach values in a range of $\gamma_{max} = 30° - 40°$, see exemplary Cao et al. [16].

In summary the draping of the auxiliary materials on doubly curved surfaces is a combination of areas where elongation and shearing allows a wrinkle-free deformation followed by areas with wrinkles. As the limits for elongation and shearing are very low, complex draping often results in widespread wrinkling of the auxiliary materials (see Fig. 1).

It is qualitatively known that the amount of wrinkles increases with a higher double curvature of the preform surface. Klose shows in his thesis [17] that wrinkles in auxiliary materials appear in a reproducible manner if the positioning of the materials is performed reproducible. However, wrinkles can highly effect the infusion process and therefore could lead to defects in the composite parts [18, 19]. Hence it is beneficial if wrinkles could be controlled, minimized or even avoided. One proposed solution is the pre-tailoring of the auxiliary materials as shown by Faber [20] for single curved preform surfaces. Different investigations were performed on the pre-tailoring of auxiliary materials for doubled-curved surfaces by Faber [12], Wandinger [21], TransTextil [22] and Girdauskaite et al. [23]. They show in different complexity that wrinkles can be avoided for the inner vacuum bag by inserting darts in the auxiliary materials. However, inserting darts is not a sufficient solution for the auxiliary materials of the outer vacuum bag as any insert needs to be reliably sealed after. In all of the studies above the position and orientation of the wrinkles was determined by reverse engineering for each specific application. But a general principle or test method to detect the appearing wrinkle pattern of auxiliary materials was not targeted and derived by that studies.

Test Methods In order to characterize the wrinkle pattern of auxiliary materials it is viable to adapt an established test method which derives the wrinkling and draping behavior of textiles or fabrics. The textile industry developed a multiplicity of test methods. In context of textile deformation, the majority of the methods determine single deformation values like the bending stiffness or the shear stiffness [24]. However, the test method of Cusick [25] which had been improved by Vangheluwe and Kiekens [26] aims the determination of the wrinkling behavior of textiles. A circular textile specimen is placed overhanging onto a plane disc. The wrinkling pattern which forms merely by gravity in the overhanging part of the specimen is detected. As a measure of drapability a relative drape coefficient, D, is calculated between 0 and 1. This allows the comparison of the draping behavior of different textiles [27]. An absolutely quantitative value of the draping behavior cannot be determined. The test method of Cusick can not be adapted to investigate the draping behavior of auxiliary materials as no relation to the deformation on a doubled-curved surface is given. Another textile test method is the PhabrOmeter introduced by Pan et al. [28]. A circular textile specimen fixed at the edge and punched with a stick in the center. Determined is the draping behavior of the textile in the free hanging area between fixation and punch [29]. As the textile is not deformed on a doubled-curved surface the test method is not adequate as well.

The most common test method for composite fibre fabrics are shearing test methods like the picture frame test [30–33]. However, Sancak [14] showed that the picture frame test is not sensitive enough to characterize the wrinkling behavior of auxiliary materials due to their comparatively higher shear stiffness. Sancak developed an out of plane deformation test for auxiliary materials which showed the potential of out of plane tests. The test was not suitable to derive a general description of the draping behavior as the deformation was not performed symmetric and asymmetric effects appeared.

In summary there are several test methods to derive aspects or values of specific draping mechanisms. However, none of the test methods is adequate to determine the specific draping behavior of the auxiliary materials for a doubled-curved vacuum bagging. It requires a test method which determines the limit as far an auxiliary material can be draped wrinkle-free through elongation or shearing before wrinkling appears. The application-oriented test method should be applicable for as many auxiliary materials with different draping mechanisms as possible. Therefore, in this paper we subsequently present our newly developed test method, which considers the auxiliary material specific draping behavior. The method

is technically implemented on the DrapeTester (by TexTechno), which is a standardized test method [34] developed to investigate the draping behavior of fibre fabrics as shown by Bardl et al. [35] and Christ et al. [36, 37].

Curvature Within this paper a theoretical description of the curvature will be used. It is given by the Gaussian curvature [38], which is used in order to characterize and quantify the double curvature of surfaces. The Gaussian curvature K can be calculated for each surface point as the product of the two main curvatures respectively the quotient of the two main radii: $K = K_1 \cdot K_2 = 1/R_1 \cdot 1/R_2$.

3 Experimental

Test Equipment To characterize the wrinkling behavior of the auxiliary materials a symmetric hemisphere punch test is performed. The DrapeTester by TexTechno is used as test equipment (see Fig. 3). A test specimen (1) can be slowly deformed by a punch geometry with a centered top (2). A clamping system consisting of clamping ring with mechanical stoppers above (3) and a circular sealing ring below locks the specimen during deformation. An optical sensor (4) measures the deformed surface geometry. The DrapeTester enables a precise, reproducible deformation (max. deformation heigth 100 mm) of clamped circular cut-pieces of fabrics (spherical diameter: 330 mm) using one hemisphere punch

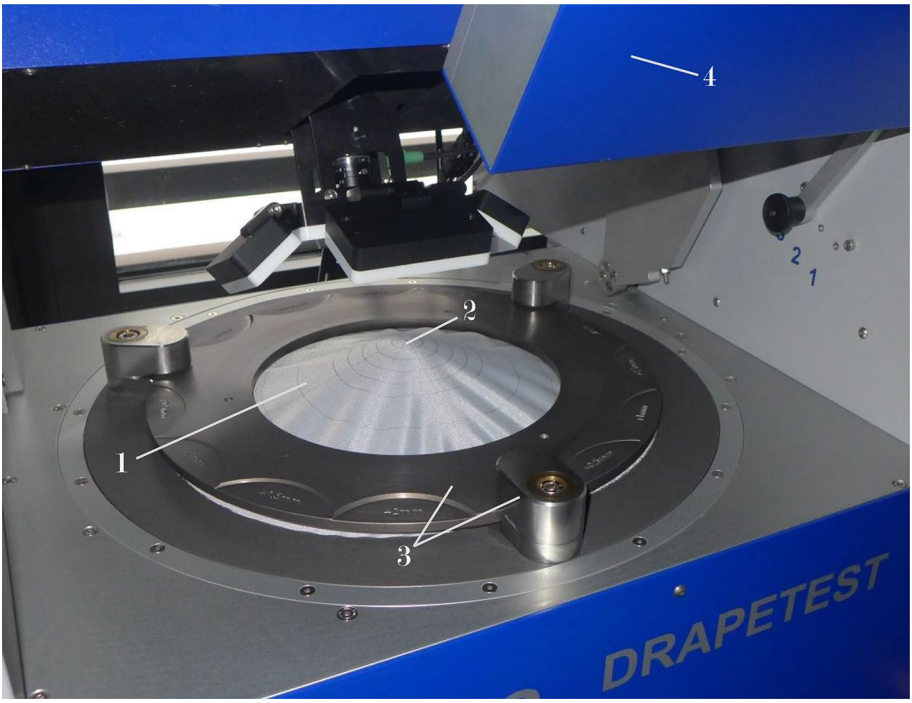

Fig. 3 Deformation test of peel ply with the test machine DrapeTester

shape (diameter: 50 mm). To measure the deformation the test equipment has the capability to measure the punch force and to map (3-D) the surface of the deformed cut-piece with an optical sensor (4).

Adjustment of the Test Method The standardized test method is designed to determine the drapability respectively the shearability of flat materials with a relatively low shear stiffness focused on dry fibre preforming (e.g. woven dry fibre fabrics). Hence adjustments were necessary in order to investigate the draping of auxiliary materials with a significantly higher shear stiffness and to additionally detect foils. First, instead of one, four hemisphere punch geometries with differing sphere radii were used. Therefore the dependency of the draping behavior on different doubled curvatures can be investigated. The radii are chosen to investigate the draping behavior on a widest range of doubled curvatures as possible. The maximum feasible punch shape diameter and the orientation of the optical sensor related to the punch shape surface are limits. Within the geometric proportions of the DrapeTester equipment the radii 50 *mm*, 75 *mm*, 100 *mm* and 200 *mm* are reasonably feasible. Figure 4 shows the four punch geometries used to deform the auxiliary materials. For the punch shapes $R = 50$ *mm* and $R = 75$ *mm* geometric transition zones (1) are necessary to fit in the DrapeTester adapter below. Tested specimens are only deformed by the hemisphere region at the top of the punch shapes and not influenced by the transition zones. Second, the functionality of the clamping ring was adjusted. In the original test method the specimens are locked during draping at the circular outer edge. This is achieved by a clamping ring with mechanical stoppers above (see Fig. 3) and a pressurized sealing ring below. For the auxiliary materials gliding during testing is required. Therefore, the pressurization of the sealing ring is deactivated and for all performed draping tests merely the net weight of the clamping ring (46 *N*) positions the specimens. Thus, a circular, uniform sliding of the auxiliary materials is enabled and plastic deformation of the auxiliary materials during the punch test are minimized. Finally, to detect and assess the draping behavior of the auxiliary materials the optical 3D surface sensor was used and the analysis routine was adjusted to detect wrinkles and wrinkle-free areas of foils and textiles.

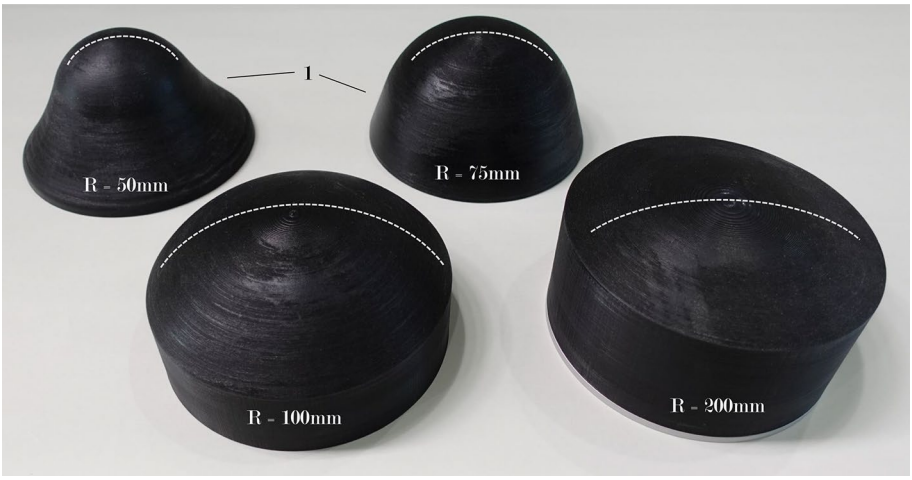

Fig. 4 Hemisphere punch shapes with different radii: 50 *mm*, 75 *mm*, 100 *mm*, 200 *mm*

Test Procedure The test specimens are circular cut-pieces of the auxiliary materials with an diameter of 330 *mm*. Circular and radial markings were added to ensure a reproducible orientation on the test machine. The test sequence was:

1. Flat and centered positioning of the specimen on the test machine with non deflected punch (punch height: 0 *mm*)
2. Placement of the clamping ring without locking the ring
3. Stepwise deflecting of the hemisphere punch shape up to an height of 100 *mm* (see Fig. 5a))
4. Detection of the deformed auxiliary material surface as a 3-D point cloud (see Fig. 5b))
5. Deduction of the centered non-wrinkled area by analyzing the 3-D mapping (see Fig. 5c) and d) and description in next paragraph)

Measurement Method The measurement aims to determine the centered, wrinkle-free area of the deformed specimen which is achievable during draping. Therefore, the position of wrinkling initiation closest to the centered top is located. Hence, the detected 3-D point cloud is geometrically superposed with the ideal hemisphere surface (see Fig. 5c)). For each point the offset directed normally to the surface is determined. At points where the offset is higher than the auxiliary material thickness, wrinkling is detected. These points are visually marked red, see Fig. 6a). Subsequently, using the shortest path (1) from the centered top (2) to the closest wrinkling point, the initial wrinkling point (3) is located. The area which is certainly drapeable wrinkle-free is represented by the spherical calotte of the ideal surface from the centered top to the initial wrinkling point. The surface area of

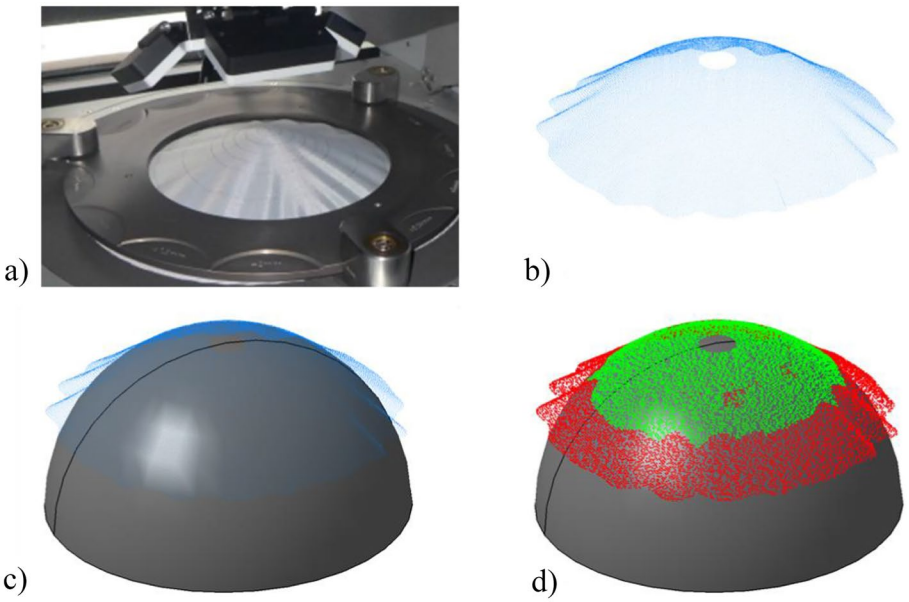

Fig. 5 Image sequence to show the measurement. **a** Punched and deformed peel ply specimen **b** Detected 3-D point cloud **c** CAD superposition of punch shape and 3-D point cloud **d** Colorization of point cloud (red: wrinkling; green: wrinkling-free)

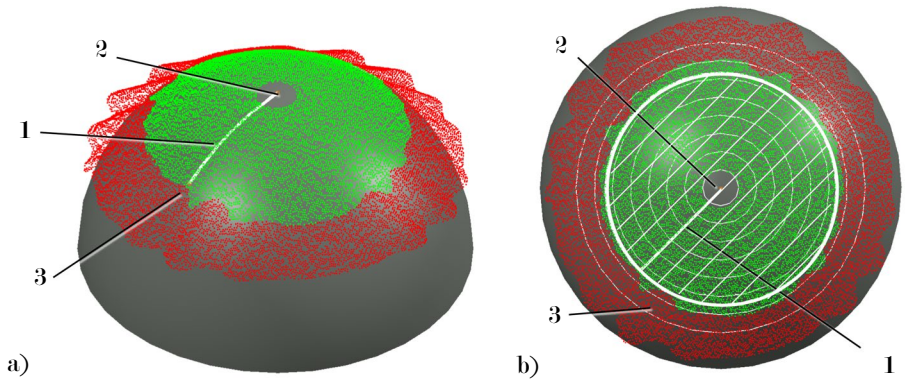

Fig. 6 Analysis of the wrinkle free area by using the shortest path (1) from the center (2) to the closest wrinkle (3). **a** Isometric view **b** Top view

the calotte $A_{calotte}$ is determined by the hemisphere radius R and the height difference h of the initial wrinkling point to the centered top: $A_{calotte} = \pi \cdot h(4R - h)$ (see shaded region in Fig. 6b)). To ensure the applicability of the measurements, the overlaying, green marked regions are neglected as they are unsteady.

Test Matrix In the study the draping behavior of different auxiliary materials, which are foils or woven fabrics, is determined. Figure 7 illustrates the considered auxiliary materials and Table 1 lists specific material data.

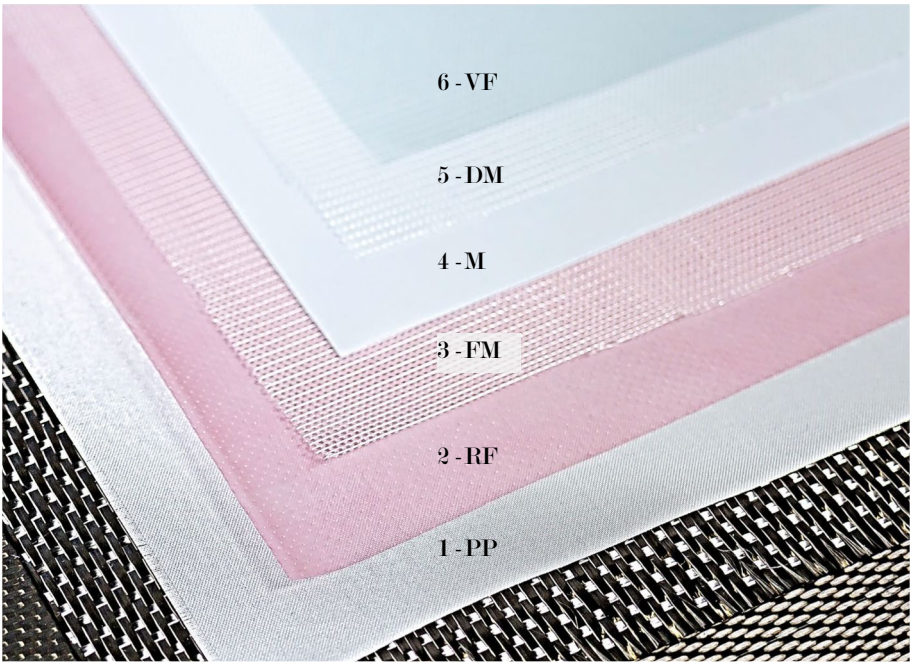

Fig. 7 Image of the considered auxiliary materials ordered in its common stacking sequence

Table 1 Definition of auxiliary materials

Aux. material	Type	Material	Thickness [mm]	Grammage [g/m^2]
Peel ply [39]	600001NAT	Woven fabric (PET)	0.14	85
Release film [40]	A6200	Perforated foil (ETFE)	0.03	30
Flow media [41]	VI5-Net	Knitted fabric (PET)	1.08	100
Membrane [42]	C2003	Woven fabric (PET)	0.13	110
Vacuum foil [43]	HS8171E	Foil (PA6)	0.05	55

Each auxiliary material was tested with each of the four hemisphere punch shapes (radii: 50 mm, 75 mm, 100 mm, 200 mm). Any test combination of auxiliary material and hemisphere punch shape was repeated three times.

4 Results

The developed test method delivers viable results and a reproducible test procedure. For every combination of auxiliary material and hemisphere punch geometry, respectively doubled curvature, measurements have been derived, except for one. The exception is the measurement of flow media with the hemisphere of $R = 200\ mm$, where the curvature is too low to form a wrinkle on the given surface area. Figure 8 shows the top view of the different auxiliary material specimens when deformed with the $R = 50\ mm$ hemisphere punch.

Figure 8a) displays a peel ply specimen in initial flat position. Figure 8b)–f) displays the different auxiliary materials in a deformed state. For each auxiliary material a uniform wrinkle pattern is identified with wrinkles running radially outward. Furthermore for each auxiliary material the centered, wrinkle-free area is identifiable and marked with a dotted line in the Fig. 8b)–f).

The surface area of these characteristic, wrinkle-free areas A_{wf} are listed in Table 2 depending on the radius of the punch geometry. It is apparent that the different auxiliary materials can be deformed wrinkle-free in different size. In increasing order these are: release film, vacuum foil, membrane, flow media, peel ply. Furthermore it is shown that the wrinkle free area A_{wf} increases with an increasing hemisphere shape radius, for each auxiliary material.

5 Discussion

The results of the tests show that the draping behavior of auxiliary materials deformed on doubled-curved surfaces can be detected. Two characteristics are identified: first a circular distributed pattern of radial wrinkles and second a centered wrinkle-free area. The second characteristic is the more usable and will be regarded in the following. As overlaying points are neglected (see measurement method in Section 3) the absolute values of Table 2 reliably represent the minimum wrinkle-free drapable areas of a material on the given surface doubled curvature. Regarding the low standard deviation (average of 6.3% and max.

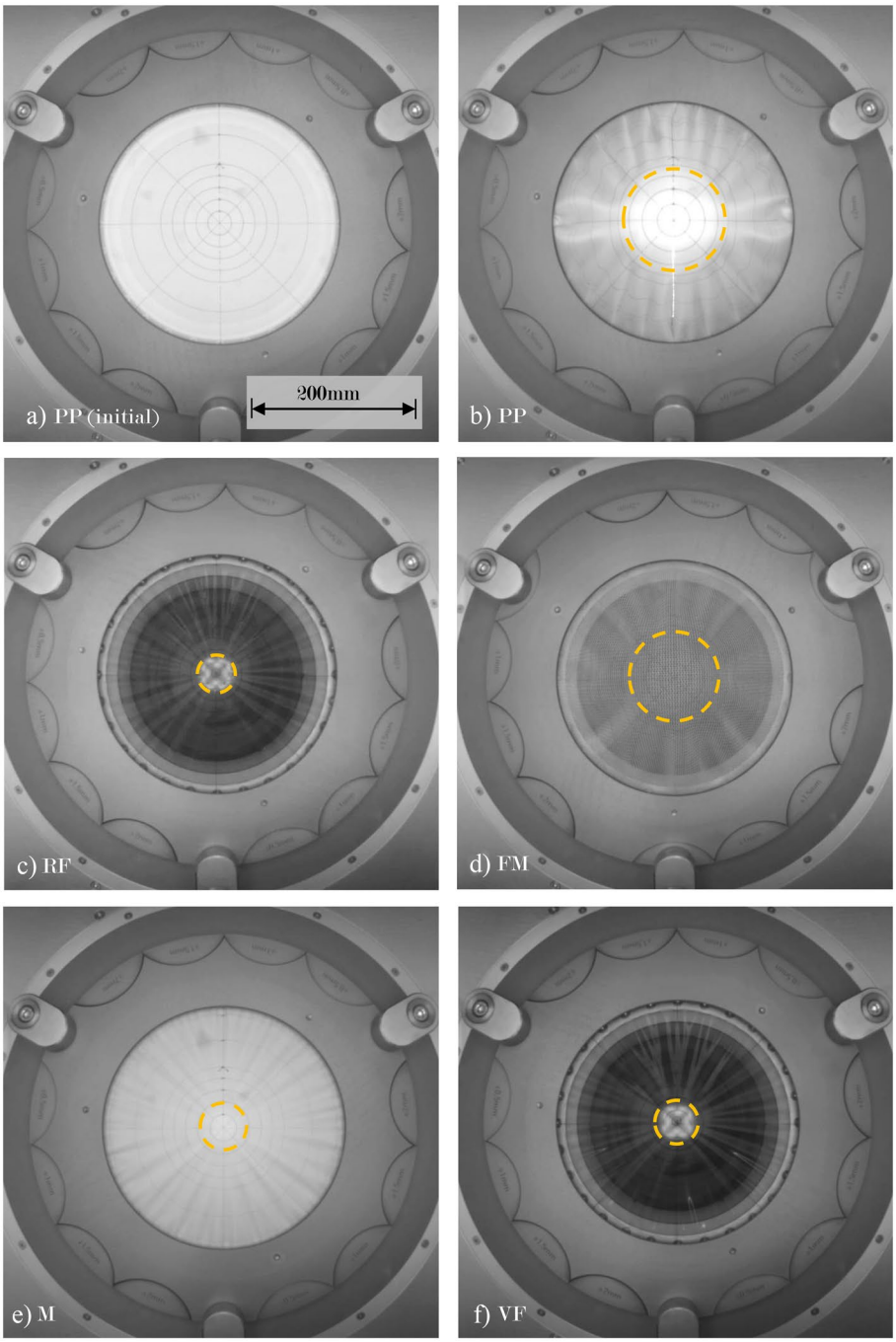

Fig. 8 Images of the punch tests in top view. **a** Peel ply specimen in initial flat position **b** Deformed peel ply specimen **c** Deformed release film specimen **d** Deformed flow media specimen **e** Deformed membrane specimen **f** Deformed vacuum foil specimen

Table 2 Test results of the deformed auxiliary materials given by the centered wrinkle-free area A_{wf} for the different diameters of the hemisphere shapes

Wrinkle-free area $[mm^2]$	$R = 50\ mm$	$R = 75\ mm$	$R = 100\ mm$	$R = 200\ mm$
Peel ply $A_{wf,PP}$	3346 ± 44	4796 ± 118	6219 ± 466	12253 ± 301
Release film $A_{wf,RF}$	588 ± 73	772 ± 123	1829 ± 88	3661 ± 144
Flow media $A_{wf,FM}$	2633 ± 106	4208 ± 194	6001 ± 234	–
Membrane $A_{wf,M}$	1041 ± 35	1735 ± 50	2183 ± 101	6081 ± 899
Vacuum foil $A_{wf,VF}$	873 ± 26	1363 ± 76	2378 ± 139	4961 ± 766

15.9% deviation of the absolute value) of the measurements indicates that this newly developed test procedure achieves reproducible and usable results.

The test method allows the comparison of the draping behavior of different auxiliary materials. Even slight differences of the deformed, wrinkle-free area of different auxiliary materials can be detected and quantified (see e.g. release film to vacuum foil). The textile fabric materials peel ply and flow media enable a wrinkle-free deformation on a significantly larger area than the foil based materials release film and vacuum foil. However, because the textile fabric material membrane is not drapable on a larger area, a simple classification of auxiliary materials by fabric textile or foil is not sufficient. Regarding to the behavior of the single auxiliary materials the results show, as expected, that the wrinkle-free area increases with an increasing radius respectively a decreasing double curvature of the hemisphere surface.

Regarding the material flow media (FM) one measurement point is missing. This fact points out, that the resolution of the test method, given by the difference of the doubled curvature of the punch shapes, should be refined in future. Thus, the test method is usable for a wider variety of material draping behaviors.

Application of the Results The experimentally derived results allow, for a tested auxiliary material, to determine the area on which it deforms with no wrinkles. For that purpose the measured results are used to derive a dependency of the deformed area and the hemisphere radius in the range of $R = 50\ mm$ to $R = 200\ mm$. In Fig. 9 the wrinkle-free area is plotted to the hemisphere radius for each auxiliary material and shows in first approximation linear dependency of the wrinkle-free area and the hemisphere radius for each auxiliary material.

This enables a practical application. For each auxiliary material the regression line represents the boundary line for wrinkle formation during the draping process. The wrinkle-free area can be determined by means of the lines, depending on the hemisphere radius. A thought experiment allows a simply applicable description. Two peel ply cut-pieces are draped on a hemisphere with $R = 150\ mm$. The area of cut-piece A is freely chosen to $A_{CutA} = 7000\ mm^2$ and for cut-piece B to $A_{CutB} = 11000\ mm^2$. These areas correspond to Cut A and Cut B in Fig. 9. As point Cut A lies under the regression line of peel ply (blue) a wrinkle-free deformation can be achieved. As point Cut B lies above, wrinkling formation needs to be expected.

The linear regression lines were determined under the assumption of a zero-crossing at $R = 0$. The assumption is justified as the area goes to zero for a radius which goes to zero. Thus, the equation $A_{wf}(R) = a_{wf} \cdot R$ is the basis of the regression lines. Table 3 shows the gradients a_{wf} for each auxiliary material with the corresponding determination coefficient R^2.

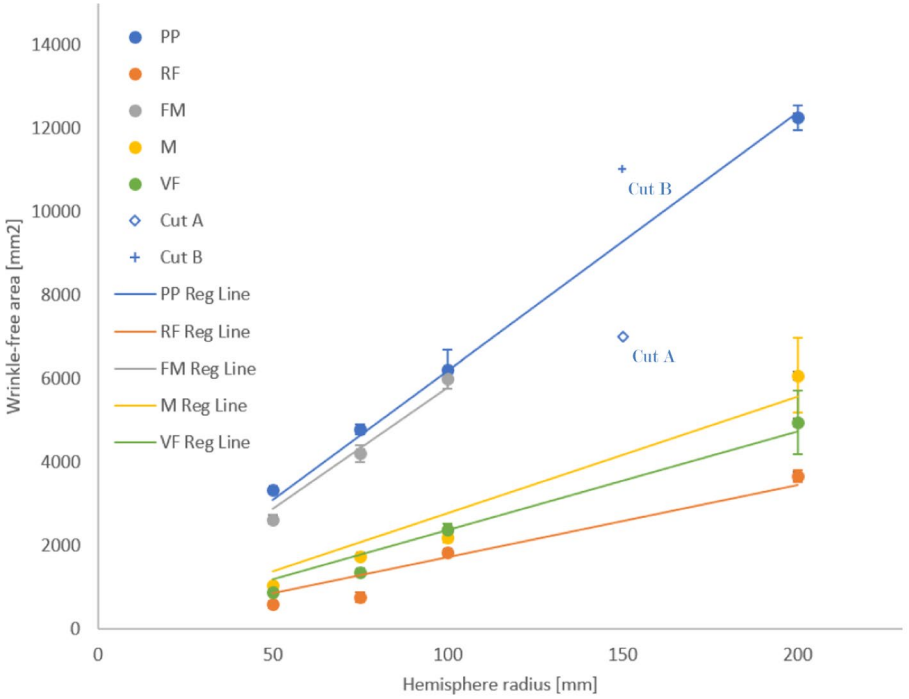

Fig. 9 Plot of the wrinkle-free area to the hemisphere radius for each auxiliary material inclusive regression lines

Approach for Generalization The represented results are based on spherical geometries. However, it is advantageous to apply the results and method for a wide variety of curved geometries in general. Therefore we suggest to consider the results depending on the double curvature of the surfaces, the Gaussian curvature K. The Gaussian curvature of a sphere is $K = 1/R^2$, thus the conversion is $R = 1/\sqrt{K}$. If R is replaced, the linear regression line is transformed to a regression curve $A_{wf}(K) = a_{wf} \cdot 1/\sqrt{K}$. The conversion of the curves equations to $a_{wf} = A_{wf}(K) \cdot \sqrt{K}$ shows the characteristic of the regression curves for each auxiliary material. The product of the wrinkle-free deformable area $A_{wf}(K)$ and the square root of the corresponding Gaussian curvature $\sqrt{K}$ is constant a_{wf} for a given auxiliary material. Figure 10 shows the plot of the scalar measurements and the corresponding regression curves in relation to $\sqrt{K}$.

Table 3 Values of the linear regression for each auxiliary material

Aux. material	a_{wf} [mm]	R^2 [-]
Peel ply [PP]	61,9	0,997
Release film [RF]	17,2	0,932
Flow media [FM]	57,8	0,977
Membrane [M]	27,8	0,943
Vacuum foil [VF]	23,7	0,968

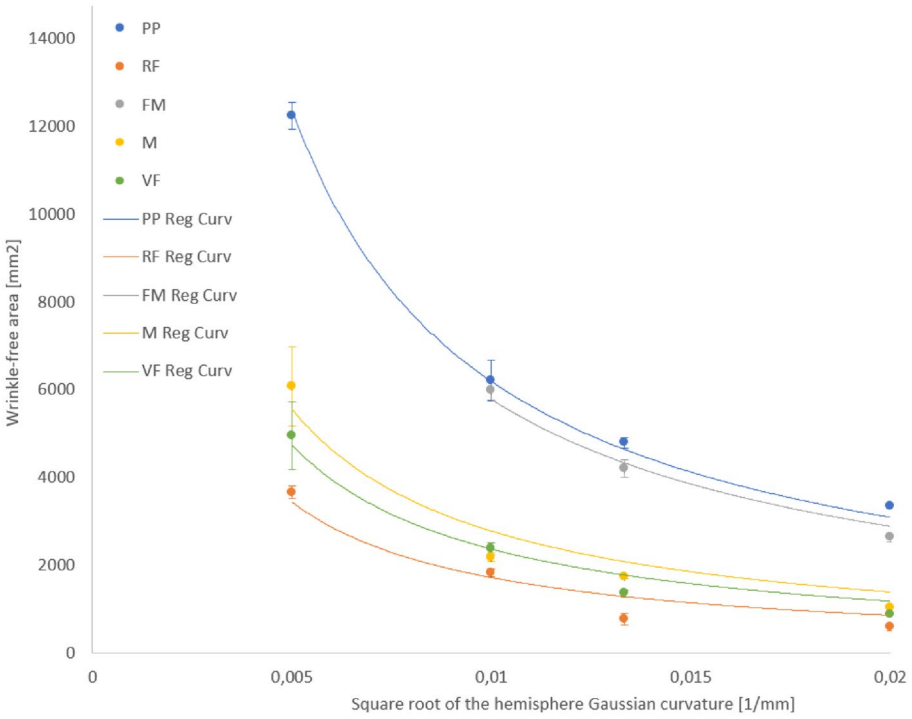

Fig. 10 Plot of the wrinkle-free area to the Gaussian curvature for each auxiliary material inclusive regression curves

Visually the area of the rectangle spanned from the origin (0/0) to any point of one curve is equal to a_{wf} for a given auxiliary material. As the regression curve represents the limit curve for a wrinkle-free drapability, the constant $a_{wf} = A_{wf}(K) \cdot \sqrt{(K)}$ may be used as scalar limit value for variable doubled-curved surfaces. For each auxiliary material the specific constant a_{wf} can be derived by the presented, newly developed hemisphere punch test method.

6 Conclusion

Auxiliary materials are often needed within the composite manufacturing where the draping quality is crucial especially on complex shaped doubled-curved surfaces. In this study we enhanced a standardized test method, focusing on the determination of the specific draping behavior of auxiliary materials. The new test method primary detects the area which is wrinkle-free drapable on different hemisphere surfaces. Consequentially limits for curvature for wrinkle-free draping can be derived in a range of a hemisphere radius from 50 *mm* to 200 *mm* for peel ply (PP), release film (RF), membrane (M) and vacuum foil (VF). Based on an unavailable measurement point for flow media (FM) (R = 200 *mm*) we recommend to increase the resolution of the test method through more punch shapes of different radii. It is shown, that for each auxiliary material the wrinkle-free area is linear linked to the

hemisphere radius (see Table 3). Subsequently the basis for the prediction of wrinkle-free areas and wrinkle appearance is given for spherical surfaces. A promising approach is discussed to directly adopt the knowledge to predict wrinkle appearance on variable doubled-curved surfaces considering the Gaussian curvature K. The test method is one of the first approaches to determine the draping behavior of auxiliary materials. Therefore the assumptions need to be refined on a wider geometric spectrum of curved surfaces, also on variably curved ones. Furthermore, the applicability of the test method to precisely determine the different draping behavior of specific auxiliary materials (e.g. different peel plies) needs to be investigated.

The gained knowledge can be advantageously used in the design of auxiliary material patterns, enabling net-shaped, pre-tailored auxiliary materials calculated by the doubled-curved surface geometry. This leads to a considerable increase of the draping reproducibility of the auxiliary materials during the vacuum bagging process. Therefore, wrinkle position and appearance can be minimized and the risk for faulty composite parts in production is reduced.

Furthermore, the gained knowledge can be potentially applied to characterize the draping behavior of material with similar properties, for example for prepregs, thermoplastics and metallic foils.

Author Contributions C.S.-E.: Conceptualization, methodology, investigation, data curation, validation, visualization, writing - original draft H.V.: Supervision, funding acquisition, writing - review M.K.: Funding acquisition, writing - review.

Funding Open Access funding enabled and organized by Projekt DEAL. The study was conducted within the research progress at the German Aerospace Center in Augsburg in a project which was funded by the Federal Ministry for Economic Affairs and Climate Action.

Data Availability No datasets were generated or analysed during the current study.

Declarations

Competing Interests The authors declare no competing interests.

References

1. Hellard, G.: Composites in Airbus. A long story of innovations and experiences. Global Investor Forum. https://docplayer.net/25342669-Composites-in-airbus-a-long-story-of-innovations-and-experiences-presented-by-guy-hellard.html (2008). Accessed 10 Nov 2023
2. Miller, A.G.: The Boeing 787 Dreamliner: More than an airplane AMTAS. https://depts.washington.edu/amtas/events/amtas_05spring/Miller.pdf (2005). Accessed 10 Nov 2023
3. Marsh, G.: Bombardier throws down the gauntlet with CSeries Airliner. Reinf. Plast. (2011). https://doi.org/10.1016/S0034-3617(11)70181-3
4. Trans Textil: VAP®: membrane-assisted low-pressure infiltration. http://www.vap.trans-textil.de/vap_process_de.html (2019). Accessed 10 Nov 2023

5. Utecht, S., Stadler, F., Filsinger, J., Lorenz, T.: Method and device for producing fiber-reinforced components by an injection method EP1420940B1. https://patentimages.storage.googleapis.com/2f/d9/15/0b971309852c10/EP1420940B1.pdf (2001). Accessed 10 Nov 2023
6. Li, W., Krehl, J., Gillespie, J.W., Heider, D., Endrulat, M., Hochrein, K., Dunham, M.G., Dubois, C.J.: Process and performance evaluation of the vacuum-assisted process. J. Compos. Mater. **38**(20), 1803–1814 (2004). https://doi.org/10.1177/0021998304044769
7. Fette, M.: Die Airbus A350-XWB-Familie im Überblick. Sonderprojekte ATZ/MTZ **24**(Suppl 2), 40–41 (2019). https://doi.org/10.1007/s41491-019-0041-z
8. Gardiner, G.: Resin Infused MS 21 Wings and Wingbox. Composite World. https://www.compositesworld.com/articles/resin-infused-ms-21-wings-and-wingbox (2014). Accessed 10 Nov 2023
9. Gardiner, G.: Bombardier wins award for resin transfer infusion wing. Composite World. https://www.compositesworld.com/news/bombardier-wins-uk-royal-academy-of-engineering-award-for-resin-transfer-infusion-wing (2019). Accessed 10 Nov 2023
10. Federation of Reinforced Plastics: Handbuch Faserverbundkunststoffe/Composites. Springer (2013). https://doi.org/10.1007/978-3-658-02755-1
11. Tiltmann, U., Utecht, S.: Schematische Darstellung VAP® - Aufbau. Composyst. https://www.composyst.com/wp-content/uploads/2023/02/COMPOSYST_Imagebroschuere_web_neu.pdf (2019). Accessed 10 Nov 2023
12. Faber, J., Schmidt-Eisenlohr, C., Dickhut, T., Ortmann, P.: Concept study on optimized auxiliary material design and application techniques for vacuum bagging of full-scale CFRP rocket boosters. In: 18th European Conference on Composite Materials. https://elib.dlr.de/120813/ (2018)
13. Breuer, U.P.: Commercial Aircraft Composite Technology. Springer Cham (2016). https://doi.org/10.1007/978-3-319-31918-6.S.91-100
14. Sancak, E.: Ermittlung von Drapierkennwerten der Vakuumaufbau-Hilfsstoffe für CFK-Strukturen mit doppelt gekrümmten Oberflüchen. Technische Hochschule Ingolstadt. https://elib.dlr.de/113477/ (2017). Accessed 16 Nov 2023
15. Shanbeh, M., Johari, M.S., Zarrebini, M., Barburski, M., Komisarczyk, A.: Analysis of shear characteristics of woven fabrics and their interaction with fabric integrated structural factors. J Eng Fibers Fabr (2019). https://doi.org/10.1177/1558925019867520
16. Cao, J., Akkerman, R., Boisse, P., Chen, J., Cheng, H.S., de Graaf, E.F., Gorczyca, J.L., Harrison, P., Hivet, G., Launay, J., Lee, W., Liu, L., Lomov, S.V., Long, A., de Luycker, E., Morestin, F., Padvoiskis, J., Peng, X.Q., Sherwood, J., Stoilova, T., Tao, X.M., Verpoest, I., Willems, A., Wiggers, J., Yu, T.X., Zhu, B.: Characterization of mechanical behavior of woven fabrics: Experimental methods and benchmark results. Compos. A Appl. Sci. Manuf. **39**(6), 1037–1053 (2008). https://doi.org/10.1016/j.compositesa.2008.02.016
17. Klose, A.: Experimentelle und theoretische Untersuchungen der Drapiermechanismen von Einzelhilfsstoffen für vakuumunterstützte Prozesse. Technical University of Chemnitz. https://elib.dlr.de/101520/ (2016). Accessed 10 Nov 2023
18. Sas, H.S., Simacek, P., Advani, S.G.: A methodology to reduce variability during vacuum infusion with optimized design of distribution media. Compos. A Appl. Sci. Manuf. **78**, 223–233 (2015). https://doi.org/10.1016/j.compositesa.2015.08.011
19. Hsiao, K.-T., Advani, S.G.: Flow sensing and control strategies to address race-tracking disturbances in resin transfer molding. Part I: Design and algorithm development. Compos. A Appl. Sci. Manuf. **35**(10), 1149–1159 (2004). https://doi.org/10.1016/j.compositesa.2004.03.010
20. Faber, J., Schmidt-Eisenlohr, C.: Automated lay-up of auxiliary materials for vacuum infusion processes. International Symposium on Composite Materials. https://elib.dlr.de/101520/ (2016). Accessed 16 Nov 2023
21. Wandinger, M.: Experimentelle Konzeptentwicklung zur Aufbringung von Hilfsstoffen für die Herstellung großflächiger, doppelt gekrümmter CFK-Raumfahrtstrukturen. Hochschule München University of Applied Sciences. https://elib.dlr.de/117656/ (2017). Accessed 16 Nov 2023
22. Trans Textil: VAP® 3D: Solutions adapted to component form. http://www.vap.trans-textil.de/vap_en.html (2015). Accessed 16 Nov 2023
23. Girdauskaite, L., Krzywinski, S., Schmidt-Eisenlohr, C., Utecht, S., Krings, M.: Introduction of Automated 3D Vacuum Buildup in the Composite Manufacturing Chain. 2nd Symposium on Automated Composite Manufacturing. https://elib.dlr.de/101522/ (2015). Accessed 16 Nov 2023
24. Cetex: ACPM 200P automatic bending stiffness testing device with parallel measurement value logging. https://www.cetex.de/fileadmin/user_upload/PDF/Produkte/ACPM_200P_eng_2020.pdf. Accessed 26 Feb 2024
25. Cusick, G.E.: The dependence of fabric drape on bending and shear stiffness. J. Text. Inst. **56**(11), T596–T606 (1965). https://doi.org/10.1080/19447026508662319

26. Vangheluwe, L., Kiekens, P.: Time dependence of the drape coefficient of fabrics. Int. J. Cloth. Sci. Technol. **5**(5), 5–8 (1993). https://doi.org/10.1108/eb003022
27. Seif, M.: Bereitstellung von Materialkennwerten für die Simulation von Bekleidungsprodukten. Technical University of Dresden. https://nbn-resolving.org/urn:nbn:de:swb:14-1187365386964-97901 (2007). Accessed 26 Feb 2024
28. Pan, N., Lin, C., Xu, J.: A new method for measuring fabric drape with a novel parameter for classifying fabrics. Preprints (2018). https://doi.org/10.20944/preprints201801.0049.v2
29. Yim, K., Kan, C.: A Comparison Study of Fabric Objective Measurement (FOM) Using KES-FB and PhabrOmeter system on warp knitted fabrics handle - smoothness, stiffness and softness. International Journal of Materials and Metallurgical Engineering **8**(8), 791–794 (2014). https://api.semanticscholar.org/CorpusID:10573048
30. Lomov, S.V., Willems, A., Verpoest, I., Zhu, Y., Barburski, M., Stoilova, T.: Picture frame test of woven composite reinforcements with a full-field strain registration. Text. Res. J. **76**(3), 243–252 (2006). https://doi.org/10.1177/0040517506061032
31. Peng, X.Q., Cao, J., Chen, J., Xue, P., Lussier, D.S., Liu, L.: Experimental and numerical analysis on normalization of picture frame tests for composite materials. Compos. Sci. Technol. **64**(1), 11–21 (2004). https://doi.org/10.1016/s0266-3538(03)00202-1
32. Harrison, P., Abdiwi, F., Guo, Z., Potluri, P., Yu, W.R.: Characterising the shear-tension coupling and wrinkling behaviour of woven engineering fabrics. Compos. A Appl. Sci. Manuf. **43**(6), 903–914 (2012). https://doi.org/10.1016/j.compositesa.2012.01.024
33. Harrison, P., Clifford, M.J., Long, A.C.: Shear characterisation of viscous woven textile composites: A comparison between picture frame and bias extension experiments. Compos. Sci. Technol. **64**(10 11), 1453–1465 (2004). https://doi.org/10.1016/j.compscitech.2003.10.015
34. DIN EN ISO 21765:2021-04 - Determination of fabric deformability by forced mechanical distension. https://www.beuth.de/en/standard/din-en-iso-21765/334972761 (2021). Accessed 08 Mar 2024
35. Bardl, G., Nocke, A., Häbner, M., Gereke, T., Pooch, M., Schulze, M., Heuer, H., Schiller, M., Kupke, R., Klein, M., Cherif, C.: Analysis of the 3D draping behavior of carbon fiber non-crimp fabrics with eddy current technique. Compos. B Eng. **132**, 49–60 (2018). https://doi.org/10.1016/j.compositesb.2017.08.007
36. Christ, M., Miene, A., Moerschel, U.: Characterization of the drapability of reinforcement fabrics by means of an automated tester. SPE Automotive Composites Conference & Exhibition. https://www.semanticscholar.org/paper/characterization-of-the-drapability-of-fabrics-by/313eec28e17d4bc7925dcd20b63db1c613d640bc#citing-papers (2012). Accessed 16 Nov 2023
37. Christ, M., Miene, A., Mörschel, U.: Measurement and analysis of drapability effects of warp-knit NCF with a standardised, automated testing device. Appl. Compos. Mater. **24**(4), 803–820 (2017). https://doi.org/10.1007/s10443-016-9555-7
38. Do Carmo, M.P.: Differential Geometry of Curves and Surfaces: Revised and Updated, 2nd edn. Courier Dover Publications, New York (2016)
39. Precision Fabrics Group: Peel ply 60001-60 NAT. Data sheet. https://www.composyst.com//download/6163/ (2020). Accessed 16 Nov 2023
40. Richmond AeroVac: Release film A6200P. Data sheet. https://www.composyst.com/download/6967/?tmstv=1688456192 (2020). Accessed 16 Nov 2023
41. Richmond AeroVac: Flow media VI5 net. Data sheet. https://www.composyst.com/download/6121/ (2020). Accessed 16 Nov 2023
42. Trans Textil GmbH: Membrane C2003. Data sheet. https://www.composyst.com//download/4256/ (2020). Accessed 16 Nov 2023
43. Richmond AeroVac: Vacuum foil HS8171. Data sheet. https://www.composyst.com//download/4534/ (2020). Accessed 16 Nov 2023